ChemComm

COMMUNICATION

View Article Online
View Journal | View Issue

The fabrication of formamidinium lead iodide perovskite thin films *via* organic cation exchange†

Zhongmin Zhou, Shuping Pang,* Fuxiang Ji, Bo Zhang and Guanglei Cui*

Cite this: *Chem. Commun.*, 2016, 52, 3828

Received 30th November 2015,
Accepted 4th February 2016

DOI: 10.1039/c5cc09873d

www.rsc.org/chemcomm

High-quality formamidinium lead iodide ($FAPbI_3$) perovskite thin films are fabricated *via* organic cation exchange. With ammonia lead iodide (NH_4PbI_3) as the starting material, the NH_4^+ in NH_4PbI_3 could be gradually substituted by FA^+ in formamidine acetate (FA-Ac) and simultaneously transformed to the pure phase α-$FAPbI_3$ at elevated temperature.

In recent years, perovskite solar cells have attracted tremendous attention due to its increasing light-to-electricity conversion efficiency. The efficiency record has been continuously broken, rocketing from 3.81% in 2009 ($CH_3NH_3PbI_3$ as the sensitizer) to 21.0% by the end of 2015 (composite perovskite as the active layer).[1,2] $CH_3NH_3PbI_3$ ($MAPbI_3$) is the pioneering material and plenty of deposition methods have been developed, such as the typical one-step solution deposition,[3] sequential deposition,[4] and other derivative techniques.[5–10] Almost all these methods start with lead halide (PbX_2) and methylammonium iodide (MAI) as the precursors.[11] In comparison to $MAPbI_3$, the more recently developed $FAPbI_3$ perovskite is less studied. The preparation of the high-quality black α-$FAPbI_3$ perovskite film is still a challenge, because the yellow δ-$FAPbI_3$ non-perovskite polymorph phase formed from one-step solution processing at room temperature is very hard to remove. The unique crystal structure character of $FAPbI_3$ is attributed to the larger ion size of FA^+ (the ionic radii of FA^+ and MA^+ are 2.79 Å and 2.70 Å, respectively) compared to MA^+.[12] Theoretically, the yellow δ-$FAPbI_3$ non-perovskite polymorph phase can transform to the photoactive black α-$FAPbI_3$ phase at elevated temperature (>140 °C). Actually, it is not easy to for δ-$FAPbI_3$ to fully transform to α-$FAPbI_3$ when it fills the scaffold layer probably because of the stress from the substrate.[13]

Among all the solution processing methods, the sequential deposition method can directly lead to the α-$FAPbI_3$ phase, but it always produces a large surface roughness because of the volume expansion behaviour and also results in the formation of some unreacted PbI_2 residues,[14] which dramatically decrease the stability of the devices.[15] The recently developed intramolecular exchange strategy by replacing the dimethylsulfoxide (DMSO) molecule with formamidinium iodide (FAI) from the DMSO–PbI_2 complex can directly produce full coverage α-$FAPbI_3$ films,[2] implying that molecule or even ion exchange may be a promising direction for the direct synthesis of α-$FAPbI_3$ without the formation of the yellow δ-$FAPbI_3$ non-perovskite polymorph.

In this communication, we presented an organic cation exchange method to directly grow α-$FAPbI_3$ perovskite films, using NH_4PbI_3 and FA-Ac as precursors using the CVD technique. NH_4PbI_3 is selected as the precursor for its high solubility in *N*,*N*-dimethylformamide (DMF). The organic cation exchange process is schematically depicted in Fig. 1. An equimolar amount of PbI_2 and NH_4I was firstly dissolved in DMF. Then the precursors were spin-coated onto the as-prepared substrate. These as-obtained films were put into the upper center of the CVD tube furnace, while FA-Ac was placed just under the films. Then the quartz tube was evacuated to under 10^{-2} Pa, and at the same time heated up to 160 °C. The black α-$FAPbI_3$ polymorph phase was obtained during the exchange process between FA^+ and NH_4^+. NH_4Ac as the product of cation exchange is more volatile than FA-Ac, which is beneficial for the occurrence of the cation exchange.

The crystal structure of the NH_4PbI_3 has been confirmed by X-ray diffraction (XRD) measurements. Fig. 2A shows the indexed XRD pattern deposited on the FTO/compact

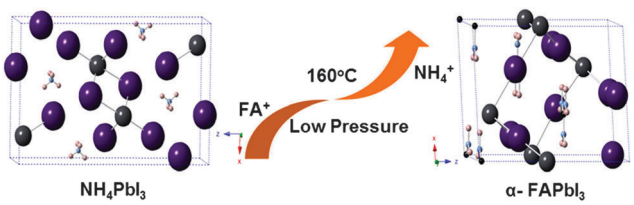

Fig. 1 Schematic illustration of the proposed cation exchange process.

Qingdao Institute of Bioenergy and Bioprocess Technology, Chinese Academy of Sciences, Qingdao 266101, People's Republic of China.
E-mail: pangsp@qibebt.ac.cn, cuigl@qibebt.ac.cn; Tel: +86-5328066-2746

† Electronic supplementary information (ESI) available: Experimental details and Fig. S1–S6 and Table S1. See DOI: 10.1039/c5cc09873d

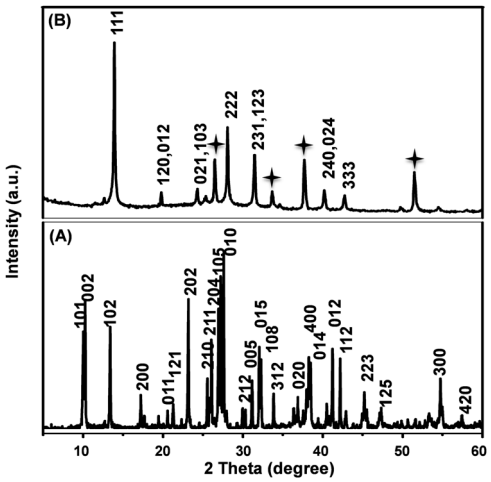

Fig. 2 XRD patterns of (A) NH_4PbI_3 and (B) $FAPbI_3$ films on the FTO/c-TiO_2/mp-TiO_2 substrate.

(c)-TiO_2/mesoporous(mp)-TiO_2 substrate. Rietveld refinement analysis of the X-ray powder diffraction pattern indicates that the synthesized NH_4PbI_3 has the lattice parameters of a = 10.308 Å, b = 4.378 Å, and c = 17.281 Å, with the space group of *Pmn*21, which is in good agreement with the reported results.[16]

The structure of α-$FAPbI_3$ was confirmed by XRD and UV-vis absorption measurements. All the peaks are in good agreement with those reported for α-$FAPbI_3$.[17] It shows that the as-prepared α-$FAPbI_3$ film has a very strong (111) orientation diffraction peak at 13.8° in comparison with the α-$FAPbI_3$ powder sample.[17] The UV-vis absorption spectra of the NH_4PbI_3 film and the film after the cation exchange process are presented in Fig. 3. They show the total absorption in the visible spectral range for the film after the reaction. The linear fits of the absorption edge of the as-synthesized α-$FAPbI_3$ film indicate that the absorption onset is *ca.* 840 nm, corresponding to a bandgap of 1.47 eV, which is close to that of the α-$FAPbI_3$ film synthesized by the two-step dipping method.[18] Compared to the 1.55 eV bandgap for $MAPbI_3$, the bandgap of α-$FAPbI_3$ is closer to the ideal bandgap for single-junction solar cells.[19]

In order to gain insight into the cation exchange process, Fourier transform infrared spectroscopy (FTIR) was used to

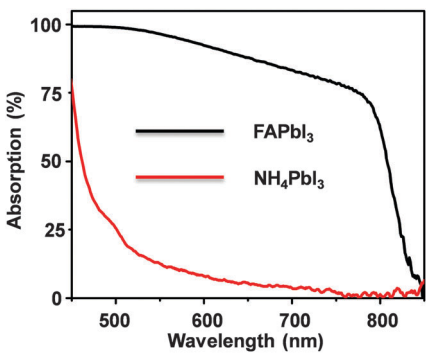

Fig. 3 UV-vis absorbance spectra of NH_4PbI_3 and α-$FAPbI_3$ films on the mesoporous-TiO_2 scaffold.

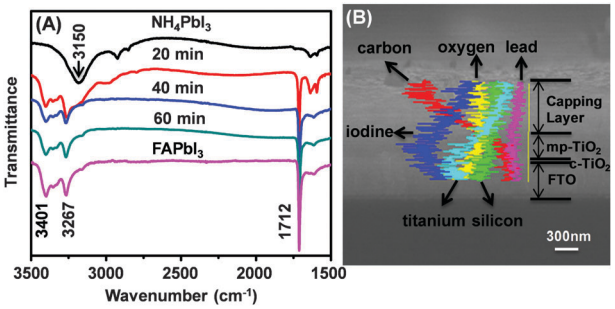

Fig. 4 (A) FTIR spectra of the prepared films with the cation exchange process for 20–60 min, and the standard $FAPbI_3$ sample, respectively. (B) SEM cross-sectional image and the EDX of an incompletely transformed $FAPbI_3$ film.

investigate the as-obtained film with different reaction times (Fig. 4A). No new stretching vibration peak of Ac^- (1540–1620 cm^{-1}) during the whole reaction process was observed,[20] which indicates that the Ac^- could not insert into the film and the cation exchange probably happens only on the film surface. We can see that a strong stretching vibration of C=N from FA^+ appears at 1712 cm^{-1} when the reaction proceeds for 20 min. At the same time, two other peaks at 3267 cm^{-1} and 3401 cm^{-1} appear, which belong to the stretching vibrations of N–H for FA^+. In addition, the stretching vibration of N–H for NH_4^+ at 3150 cm^{-1} almost disappears at 40 min. This FTIR spectrum is similar to that of the standard $FAPbI_3$ perovskite film.[21] The absorption peaks indicate that the cation exchange process was complete at ~40 min and no more FA^+ could be inserted into the starting film by extending the reaction time.

To clearly check the gradual change of composition during the ion exchange reaction, a thicker NH_4PbI_3 film was deposited for the cross-sectional measurements. The energy-dispersive X-ray (EDX) spectra of the film after the reaction proceeded for 10 min are shown in Fig. 4B. Two elements which change more obviously are carbon and iodine. There is no carbon in the NH_4PbI_3 precursor film; therefore, the appearance of carbon is attributed to the replacement of NH_4^+ with FA^+. The high concentration of FA^+ near the surface further indicates that the substitution of NH_4^+ with FA^+ occurs at the film surface. Compared with the carbon element, the opposite trend of iodine in the film is because of the relatively high iodine concentration in NH_4PbI_3 compared with that in $FAPbI_3$.[16,17] Based on the above analysis, we can surmise that the cation exchange between FA^+ and NH_4^+ occurs at the film surface, then the FA^+ ions could diffuse inside and the NH_4^+ ions diffuse to the surface and sequentially exchange with FA^+. The inside diffusion and surface ion exchange are carried out simultaneously until all the NH_4^+ ions are exchanged with FA^+ ions.

Solar cells based on the as-prepared α-$FAPbI_3$ were constructed using mp-TiO_2 as the electron transport layer and 2,2′,7,7′-tetrakis-(*N*,*N*-di-*p*-methoxyphenylamine)-9,9′-spiro-biofluorine (spiro-OMeTAD) as the hole transport layer (Fig. 5A). Dense, uniform and black films are obtained at 160 °C for a reaction time of 60 min as can be seen from the scanning electron microscopy (SEM) image in Fig. 5B. The AFM topographical image

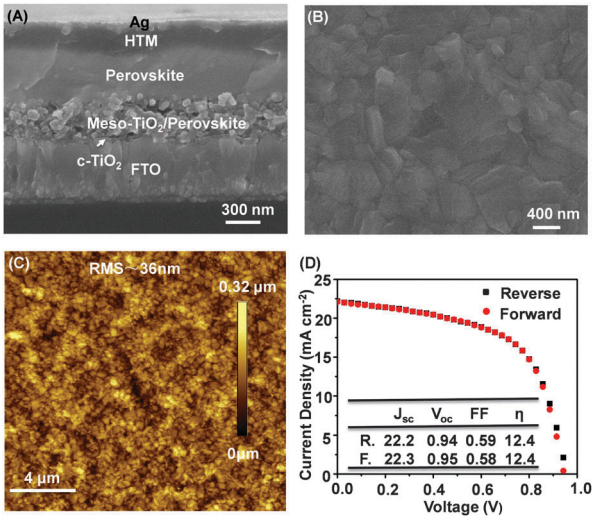

Fig. 5 (A) Cross-sectional SEM image of a complete perovskite device composed of FTO, compact blocking layer TiO_2, mesoporous-TiO_2, the perovskite film, a hole transporting layer (Spiro-MeOTAD), and a silver top electrode. (B) SEM images of the $FAPbI_3$ perovskite film. (C) AFM image of the top surfaces of the $FAPbI_3$ film. (D) J–V characteristics of a $FAPbI_3$ champion device. Inset shows the detailed photovoltaic parameters.

(20×20 μm^2) of the α-$FAPbI_3$ reveals a root mean square (RMS) roughness of approximately 36 nm (Fig. 5C). The photocurrent density as a function of bias voltage is measured under standard AM 1.5 sunlight at a humidity of about 30%. Fig. 5D shows the values of the champion device with the reverse scanning direction (from the open-circuit voltage (V_{oc}) to the short-circuit current (J_{sc})) and forward scanning direction (from J_{sc} to V_{oc}). The device exhibits an efficiency of 12.4% with no hysteresis. The statistics of PCEs are presented in Fig. S1 (ESI†), showing the high reproducibility of the cation exchange method. For comparison, the $FAPbI_3$ and $MAPbI_3$ devices are also fabricated and measured as shown in Fig. S2 and Table S1 (ESI†), indicating that the proposed cation exchange method is a viable approach towards preparation of high-quality $FAPbI_3$ perovskite films.

Other than the extended light absorbance range, the α-$FAPbI_3$ film also delivers an improved thermal stability. Fig. 6 shows the thermal stability comparison between the α-$FAPbI_3$ and $MAPbI_3$ films. Both of the films were obtained using the CVD method (the preparation procedure of the films of $MAPbI_3$ can be seen in the ESI†). A series of α-$FAPbI_3$ and $MAPbI_3$ films (without HTM and electrodes) were heated at 140 °C in an argon-filled glove box for 1–7 h. Then the corresponding devices were assembled and studied. The PCEs of α-$FAPbI_3$-based cells decreased only *ca.* 5% when the perovskite film was heated to 140 °C for up to 7 h, while the $MAPbI_3$-based devices decrease to *ca.* 11% after heating for 4 h and to zero after heating for 6 h. As shown in Fig. S3 (ESI†), the $MAPbI_3$ phase begins to decay after heating for 4 h and completely decomposed after heating for 7 h. However, the colour of the α-$FAPbI_3$ film stays almost the same even after heating for 7 h. The SEM images in Fig. 6(B, C) and Fig. S4 (ESI†) show the change of the morphology of the films

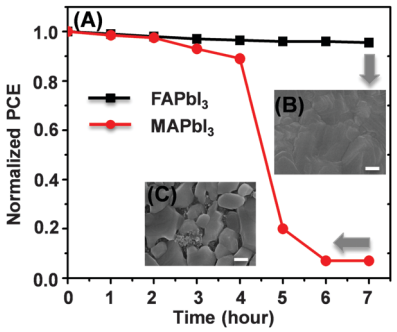

Fig. 6 (A) Normalized PCE evolution based on α-$FAPbI_3$ and $MAPbI_3$ films annealed at 140 °C for 0–7 h. (B and C) SEM images of the $FAPbI_3$ and $MAPbI_3$ films heated for 7 h. The scale bar is 200 nm.

before and after long-time heating treatment. In contrast to the stable α-$FAPbI_3$, the $MAPbI_3$ films obviously shrink after heating for 7 h.

Moreover, the presented cation exchange method was also performed on $HPbI_3$ and $MAPbI_3$ films. $HPbI_3$ was prepared according to a reported procedure,[22] and the preparation procedure of $MAPbI_3$ films can be seen in the ESI.† The XRD patterns (Fig. S5, ESI†) and the UV-vis absorption spectra (Fig. S6, ESI†) strongly confirm the successful fabrication of the $FAPbI_3$ films.

In conclusion, we have demonstrated an organic cation exchange concept for the preparation of high-quality α-$FAPbI_3$ films using the CVD method. The PCE of the champion device was 12.4% based on the mesoscopic structure with no hysteresis. We also demonstrated that this cation exchange concept could also be used to prepare α-$FAPbI_3$ thin films by replacing H^+ and MA^+ in $HPbI_3$ and $MAPbI_3$ with FA^+. This concept will be an alternative route for the development of highly efficient $FAPbI_3$ solar cells.

The financial support of this research by the International S&T Cooperation Program of China (2015DFG62670), the Chinese National Natural Science Foundation (51302279), the China Postdoctoral Science Foundation (2015M582156), the Basic Research Program of Qingdao (14-2-4-8-jch), and the Qingdao Key Lab, for solar energy utilization and energy storage technology, is greatly acknowledged.

Notes and references

1 A. Kojima, K. Teshima, Y. Shirai and T. Miyasaka, *J. Am. Chem. Soc.*, 2009, **131**, 6050–6051.
2 NREL, www.nrel.gov/ncpv/images/efficiency_chart.jpg, 2015.
3 H. S. Kim, C. R. Lee, J. H. Im, K. B. Lee, T. Moehl, A. Archioro, S. J. Moon, R. Humphry-Baker, J. H. Yum, J. E. Moser, M. Grätzel and N. G. Park, *Sci. Rep.*, 2012, **2**, 591.
4 J. Burschka, N. Pellet, S. J. Moon, R. Humphry-Baker, P. Gao, M. K. Nazeeruddin and M. Grätzel, *Nature*, 2013, **499**, 316–319.
5 M. Liu, M. B. Johnston and H. J. Snaith, *Nature*, 2013, **501**, 395–398.
6 Q. Chen, H. Zhou, Z. Hong, S. Luo, H. S. Duan, H. H. Wang, Y. Liu, G. Li and Y. Yang, *J. Am. Chem. Soc.*, 2014, **136**, 622–625.
7 S. Ahmad, P. K. Kanaujia, W. Niu, J. J. Baumberg and G. V. Prakash, *ACS Appl. Mater. Interfaces*, 2014, **6**, 10238–10247.
8 M. Xiao, F. Huang, W. Huang, Y. Dkhissi, Y. Zhu, J. Etheridge, A. Gray-Weale, U. Bach, Y. B. Cheng and L. Spiccia, *Angew. Chem., Int. Ed.*, 2014, **53**, 9898–9909.

9 A. Mei, X. Li, L. Liu, Z. Ku, T. Liu, Y. Rong, M. Xu, M. Hu, J. Chen, Y. Yang, M. Grätzel and H. Han, *Science*, 2014, **345**, 295–298.
10 K. Hwang, Y. S. Jung, Y. J. Heo, F. H. Scholes, S. E. Watkins, J. Subbiah, D. J. Jones, D. Y. Kim and D. Vak, *Adv. Mater.*, 2015, **27**, 1241–1247.
11 P. Gao, M. Grätzel and M. K. Nazeeruddin, *Energy Environ. Sci.*, 2014, **7**, 2448–2463.
12 A. Binek, F. C. Hanusch, P. Docampo and T. Bein, *J. Phys. Chem. Lett.*, 2015, **6**, 1249–1253.
13 Z. Wang, Y. Zhou, S. Pang, Z. Xiao, J. Zhang, W. Chai, H. Xu, Z. Liu, N. P. Padture and G. Cui, *Chem. Mater.*, 2015, **27**, 7149–7155.
14 L. Hu, J. Peng, W. Wang, Z. Xia, J. Yuan, J. Lu, X. Huang, W. Ma, H. Song, W. Chen, Y. B. Cheng and J. Tang, *ACS Photonics*, 2014, **1**, 547–553.
15 F. Liu, Q. Dong, M. K. Wong, A. B. Djurišic, A. Ng, Z. Ren, Q. Shen, C. Surya, W. K. Chan, J. Wang, A. M. C. Ng, C. Liao, H. Li, K. Shih, C. Wei, H. Su and J. Dai, *Adv. Energy Mater.*, 2016, 1502206.
16 L. Q. Fan and J. H. Wu, *Acta Crystallogr.*, 2007, **E63**, i189.
17 S. Pang, H. Hu, J. Zhang, S. Lv, Y. Yu, F. Wei, T. Qin, H. Xu, Z. Liu and G. Cui, *Chem. Mater.*, 2014, **26**, 1485–1491.
18 T. M. Koh, K. Fu, Y. Fang, S. Chen, T. C. Sum, N. Mathews, S. G. Mhaisalkar, P. P. Boix and T. Baikie, *J. Phys. Chem. C*, 2014, **118**, 16458–16462.
19 G. E. Eperon, S. D. Stranks, C. Menelaou, M. B. Johnston, L. M. Herz and H. J. Snaith, *Energy Environ. Sci.*, 2014, **7**, 982–988.
20 M. Luo, P. Guan and W. Liu, *Spectrosc. Spectral Anal.*, 2007, **27**, 250–253.
21 S. Wozny, M. Yang, A. M. Nardes, C. C. Mercado, S. Ferrere, M. O. Reese, W. Zhou and K. Zhu, *Chem. Mater.*, 2015, **27**, 4814–4820.
22 F. Wang, H. Yu, H. Xu and N. Zhao, *Adv. Funct. Mater.*, 2015, **25**, 1120–1126.